Nutrient removal and biodiesel feedstock potential of green alga UHCC00027 grown in municipal wastewater under Nordic conditions

Mikael Jämsä[a,+], Fiona Lynch[a,+], Anita Santana-Sánchez[a], Petteri Laaksonen[b], Gennadi Zaitsev[b], Alexei Solovchenko[c], Yagut Allahverdiyeva[a*]

[a] Molecular Plant Biology, Department of Biochemistry, University of Turku, FI-20014, Turku, Finland

[b] Clewer Ltd, Biolinja 12, FI-20750, Turku, Finland

[c] Department of Bioengineering, Faculty of Biology, Lomonosov Moscow State University, 119234 Moscow, Russia

[+] these authors have equal contribution

* corresponding author:

Y. Allahverdiyeva, Molecular Plant Biology, Department of Biochemistry, University of Turku, FI-20014, Turku, Finland, allahve@utu.fi

Abstract

Integrating cultivation with wastewater treatment improves the economics of microalgal based biofuel production and allows for the sustainable reuse of nitrogen (N) and phosphorus (P) from waste streams. Batch-cultivation of a locally isolated green microalga, UHCC00027, and an indigenous algal-bacterial consortium was undertaken on screened municipal wastewater in 24 L pilot reactors. Evaluations of growth and of N and P removal were performed at different Chemical Oxygen Demand (COD) levels and N:P ratios. Lipid accumulation and fatty acid composition of the resulting biomass were also examined. Unique to the present study was the evaluation of wastewater treatment performance under cold temperatures (7−13 °C) typical of a Nordic climate. Whilst temperature exerted little influence on heterotrophic COD removal, vigorous (temperature dependent) growth of microalgae was important in the efficient removal of N and P, with the N:P ratio playing a central role. The studied cultivation regime and organisms achieved regulatory N and P removal levels with a hydraulic retention time (HRT) of 14 days. However, biodiesel properties of the resulting biomass did not meet international standards due to a high proportion of polyunsaturated fatty acids. Possible workarounds for simultaneously increasing nutrient removal efficiency, biomass productivity, and improving biomass suitability for biodiesel under a Nordic climate are discussed.

Keywords: microalgae, biofuel, wastewater, biodiesel, nutrient removal, cold climate

1. Introduction

A transition to sustainably produced biofuels is important in meeting recently agreed global climate change targets [1,2]. Major drawbacks of 1st generation biofuels, including starch based ethanol and vegetable biodiesel, include competition over arable land and CO_2 emissions generated throughout the supply chain, limiting their sustainable production [3]. Algae-derived biodiesel is a 3rd generation biofuel and is advantageous in its non-arable production and rapid biomass generation [4]. However, chemical nutrients can constitute up to 10% of the total costs of microalgal biofuel production [5]. These costs can be mitigated by exploiting the nutrients readily available in wastewater. Municipal wastewater is generally rich in nitrogen (N) and phosphorous (P), which are necessary macro-nutrients for microalgae. Apart from nutrient removal, microalgae can also be utilized for the removal of heavy metals and organic pollutants, including hormones and other pharmaceuticals [5,6].

The current popularity of the 'circular economy' approach to integrated wastewater treatment and biofuel production is evidenced by recent microalgal based pilot projects [7–9]. However, such approaches are not generally considered favorable in Nordic countries, due to low annual light intensities and low average temperatures [10,11]. Despite this, a few studies performed on laboratory scale have demonstrated the potential for cold-tolerant strains in wastewater treatment applications [12-14].

Microalgae hold great potential as a feedstock for biodiesel (as well as for other biofuels) since their oil yield is an order of magnitude higher than that of conventional oleaginous plants. Indeed, microalgal cells can accumulate lipids at up to 80% of their dry weight [15]. Unfortunately, high lipid accumulation in microalgae usually takes place under an environmental stress such as nutrient starvation, which slows down cell

division and impairs biomass productivity. This complicates the achievement of high biomass productivity and high lipid yield in a one-stage process [16]. Possible workarounds include the development of two-stage processes (rapid growth in the first stage and stress for lipid accumulation in the second), and engineering strains with high lipid yields without sacrificing the biomass yield [17].

In evaluating the potential of different microalgal strains, it is important to note that not all lipids are equally suitable for the production of biodiesel. Generally, biodiesel from microalgae is comparable with that obtained from other sources, such as oleaginous plants, in that it has relatively low oxidative stability due to a high degree of unsaturation. This can be amended by blending the biodiesel with fossil diesel and/or chemical stabilizers [18-20]. In regions of cold climate, the temperature-related properties of diesel e.g. cloud point and cold filter plugging point become crucial for optimal fuel performance [21]. Other important properties include: the energy content, providing the inherent value of the fuel; water and acid contents, which determine the corrosive effects of the fuel; and viscosity, which determines the efficient operation of the engine [19].

In this study, we continue work with a Finnish isolate of the Scenedesmaceae family, UHCC0027. This alga was selected previously on the basis of its superior laboratory scale performance over other native strains of microalgae in nutrient removal, biomass and lipid accumulation [14]. To the best of our knowledge, this is the first pilot scale report on integrated wastewater treatment and biodiesel production of a native cold-climate alga, using real wastewater under cold climate conditions.

2. Materials and methods

2.1 Pre-cultures and inoculation of the PBRs

The chlorophyte UHCC00027 employed in this study was previously described in Lynch et al. [14]. For experiments performed at ambient temperatures typical of the Nordic summer (18–25 °C), axenic pre-cultures were grown in 5 L Erlenmeyer flasks aerated with atmospheric air at a rate of 4 L min^{-1}. The cells were batch-grown in synthetic wastewater [14] for 10 days at 22 °C under 14:10 (light:dark) photoperiod (light intensity 225 µmol PAR m^{-2} s^{-1}). For the experiment simulating cold season temperatures, the pre-cultures were grown at 6 °C under the same illumination conditions. The pre-cultures were harvested by centrifugation (6000 × *g*, 10 min) and, based on cell counting with a Bürker hemocytometer, normalized to 1.6×10^6 cells mL^{-1} (0.45 µg mL^{-1} Chl) in each of the reactors. Growth was followed using total chlorophyll (Chl) measurements performed according to Porra et al. [22]. In the blank (unseeded) wastewater, total Chl starting concentration was below 0.02 µg mL^{-1}.

2.2 Pilot-scale experiments

Five pilot scale experiments were performed in photobioreactors (PBR) at Clewer Technology Oy facilities using screened municipal wastewater (mWW) from the suburb of Varissuo (Turku, Finland). Conditions are summarized in Table 1 and Fig. S2. The wastewater used to fill the reactors differed in composition depending on the season (late spring or summer) and the time of day. This resulted in wastewater samples being characterized either by a higher COD and lower nitrogen (designated as HC_LN) or lower COD, higher nitrogen (LC_HN) content (Table 1). The LC_HN wastewater type was also tested under cold temperature, by placing a PBR in an air conditioned cold room (referred to as LC_HN cold, see also Fig. S2).

Table 1

Pilot-scale experimental conditions in PBRs for wastewater of the composition: High COD, Low N (HC_LN); Low COD, High N (LC_HN); and Low COD, High N operated under cold temperature (LC_HN cold). Values marked NM were not measured.

	HC_LN	**LC_HN**	**LC_HN cold**
Wastewater collection (season and time)	Spring, afternoon	Summer, morning	Summer, morning
Reactor fill volume (L)	24	24	24
Operating temp. range (°C)	16−26	22−29	7−13
Average operating temp. (°C)	22.8	25.5	8.3
Air flow rate (v v^{-1} min^{-1})	0.625	0.625	0.625
Light period (light:dark)	14:10	14:10	14:10
Light intensity (µmol m^{-2} s^{-1})	250	250	250
COD dissolved (mg L^{-1})	490	84	84
COD-total (mg L^{-1})	560	600	600
NH_4^+-N (mg L^{-1})	42	56	56
NO_3^--N (mg L^{-1})	0.4	0.4	0.4
NO_2^--N (mg L^{-1})	< 0.15	< 0.15	< 0.15
Total-N dissolved (mg L^{-1})	NM	59	59
PO_4^{3-}-P (mg L^{-1})	4.5	5.4	5.4
Total-P dissolved (mg L^{-1})	NM	6.1	6.1
N:P (molar ratio)	20.6	22.9	22.9

2.2.1 Pilot-scale reactor and illumination set-up

Pilot-scale (24 L) reactors (provided by Clewer Technology Oy, see Fig. S1) were cylindrical (40 cm diameter, 20 cm length). At both ends of each cylinder was a 1cm thick transparent window (diameter 30 cm). Reactors had a perforated stainless steel internal wall facilitating the even distribution of nutrients and cells in the reactor, which was continuously mixed by airlift (15 L min^{-1}, atmospheric air). Both ends of each reactor were illuminated using a 125 W CFL-Lamp (LUMii, UK, color temperature

126 6400K). Lamps were positioned 10 cm away the reactor windows. Light intensity
127 immediately inside the reactors was 250 μmol m^{-2} s^{-1}. Ambient and liquid phase
128 temperatures were monitored using a Fluke 54II thermologging device.

129 **2.2.2 Growth monitoring and wastewater analysis**

130 Growth was monitored using total Chl [21] and dry biomass weight. Dry weight was
131 measured according to the APHA method 8111G, [23] with a modified drying
132 temperature (105 °C) and filter (Whatman GF/C, 1.2 μm). Specific growth rates were
133 calculated from the linear portion of natural log transformed Chl data [24]. All nutrient
134 and COD measurements were made using the Hach Lange LCK cuvette test series
135 according to the manufacturer's protocol (LCK304 for NH_4^+-N, LCK341 for NO_2^--N,
136 LCK339 for NO_3^--N, LCK138 and LCK338 for total N, LCK349 for PO_4^{3-}-P and total-
137 P, LCK314 and LCK114 for COD). Before the measurements, the samples were filtered
138 through 0.45 μm (Sartorius, ministart, type 16537) filters. Dissolved inorganic nitrogen
139 (DIN) levels were calculated as the sum of NH_4^+-N, NO_2^--N and NO_3^--N. Interference
140 of NO_2^--N meant levels of NO_3^--N were approximated as average values using
141 uncertainty plots, whereby the maximum values were measured NO_3^--N levels and
142 minimum values were calculated according to:

143 $$NO_3^- - N(\text{min/max}) = [NO_3^- - N] - X([NO_2^- - N] \quad \text{Eq. 1}$$

144 Equation 1 was formulated based on the relationship between NO_2^--N and NO_3^--N when
145 increasing concentrations of NO_2^--N were added to wastewater samples with known
146 concentrations of NO_3^--N. In Eq.1, X is 0.2444 for the NO_3^--N minimum value and
147 0.2012 for the NO_3^--N maximum value (refer S4, S5).

2.3 Lipid and fatty acid composition analysis

Lipid analysis was performed for the LC_HN reactors only, this was so that concomitantly operated cold and room temperature reactors could be compared. Total cell lipid content and fatty acid (FA) profiles were determined in the pre-cultures (control or day 0), in the middle-exponential (days 5 and 10 for the ambient-temperature and the cold experiments, respectively) and at the late exponential phase (days 14 and 28 for the ambient-temperature and the cold experiments, respectively). The samples were vacuum-filtered through 20 µm nylon membrane filters (Sterilitech, USA), biomass was harvested by centrifugation of the filtrate (6000 × *g*, 10 min) and frozen in liquid nitrogen. The frozen biomass was lyophilized using a Flexi-dry µP (FTS systems, USA) freeze dryer for total lipid and FA analysis. Total lipids were quantified gravimetrically as described by Ryckebosch et al. [25] with a re-extraction step. Samples were analyzed in triplicate where biomass was sufficient.

For FA profile determination, *in situ* transesterification was performed according to Van Wychen and Laurens [26]. The Fatty Acid Methyl Esters (FAME) were separated on an Agilent 7890C GC equipped with an Agilent Innowax 19091N-213 (30 m × 0.32 mm × 0.5 µm) column (Agilent) and detected by 5975C inert MS (Agilent, USA). One microliter of the samples or standards were injected in splitless mode with helium carrier gas flowing at 1.4 mL min^{-1} and separated using a gradient program (50 °C for 8.5 min, ramping to 250 °C at 15 °C min^{-1}, and a final hold at 250 °C for 8 min).

FA identifications were confirmed using a standard FAME mixture (37 FAME mixture, 18919 AMP, Supelco). Quantification was performed using methods described previously [26,27], with the exception of the C16:4 FA. The C16:4 FA was quantified

using the 4(Z), 7(Z), 10(Z), 13(Z)-hexadecatetraenoic acid-d_5 standard (C16:4, Cayman Chemical) and the esterification efficiency, which was determined using stearidonic acid and stearidonic methyl ester standards (C18:4 FA and C18:4me, Cayman Chemical).

Biodiesel properties were estimated by applying the equations reported in Talebi et al. [28]. Oxidative stability was estimated according to the formula of Park et al.[29].

2.4 Statistical analysis

Pilot reactors were monitored on an approximately daily basis. An unseeded, control reactor was operated to separate the effect of seeding alga UHCC0027 from independent processes. Growth was monitored using single biomass measurements and total chlorophyll (Chl). Chl and wastewater analyses were performed as single measurements, with duplicate measurements performed approximately every 2^{nd} day to ensure technical reproducibility. Reproducibility was tested in Excel using paired student t tests. There was no significant difference found between duplicates over single test types ($P = 0.08 – 0.97$); over all Chl analyses ($P = 0.84$); or over all wastewater analyses ($P = 0.31$). Data are presented as either single measurements, or as the average and standard deviation of duplicate measurements (refer to Figs. 1 and 2 for details). Lipid and FA analysis were performed as triplicate (technical) measures, unless there was insufficient biomass, and data are presented as averaged results with standard deviations (for details, see Fig. 4).

3. Results & Discussion

3.1 Wastewater treatment and biomass accumulation

3.1.1 Growth of alga UHCC0027

The UHCC0027 cells grew slightly faster in the PBR with the higher COD, lower N (HC_LN) wastewater than in the lower COD, higher N reactor (LC_HN) (Chl accumulation kinetics, Fig. 1A). Both wastewater types clearly contained a sufficient amount and appropriate balance of nutrients to support microalgal growth, at least for the first 10 days of the experiment.

Interestingly, there was a detectable Chl accumulation in the blank LC_HN PBR which was unseeded (LC_HN blank; Fig. 1A, curve *2*). The morphology of the indigenous cells responsible for this rise indicated the presence of several types of colonial and unicellular chlorophytes, including diatoms, (Fig. S3). In the reactors seeded with the UHCC0027 alga, a small number of diatoms were observed (Fig. S3A) but they did not proliferate to a significant extent (refer S3D).

Although it was initially much lower, the rate of Chl accumulation in the unseeded LC_HN PBR eventually matched that of the corresponding seeded PBR (cf. curves *1* and *2* in Fig. 1B). Interestingly, in the first 14 days of the experiment, the seeded cold PBR exhibited kinetics of Chl accumulation similar to that of unseeded room-temperature HC_LN culture (cf. curves *2* and *5* in Fig. 1B).

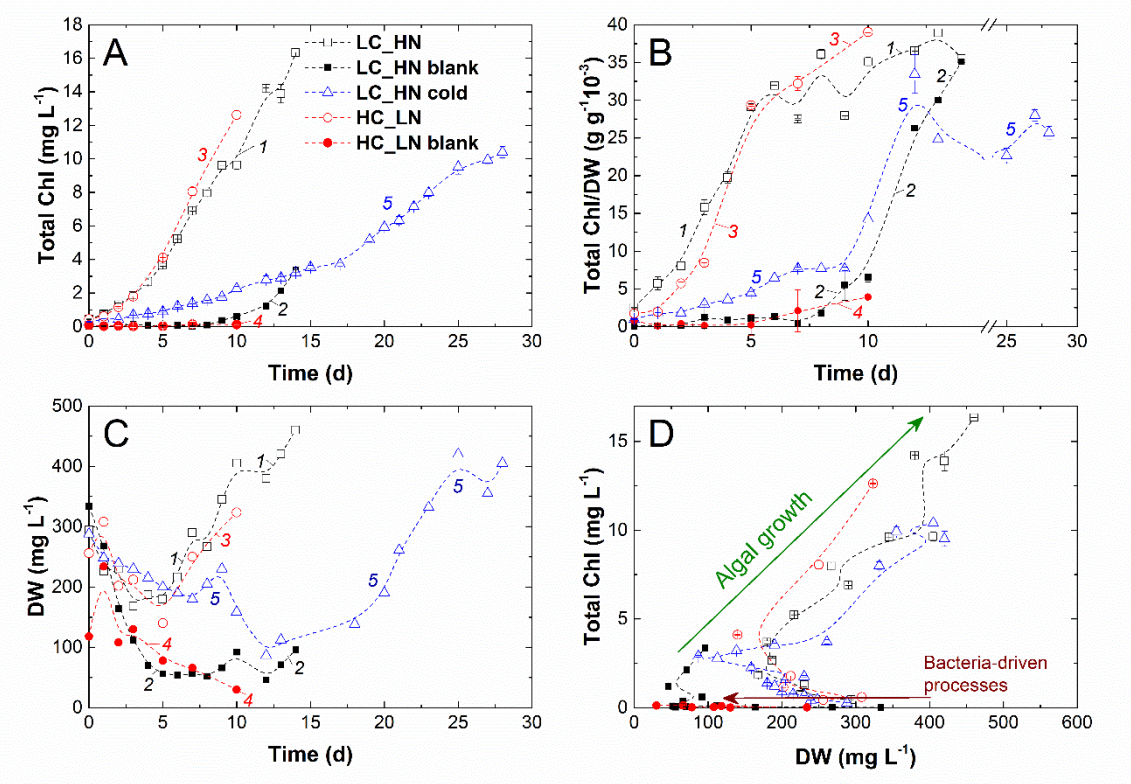

210

211 **Fig. 1.** Kinetics of total chlorophyll accumulation per unit volume (A) of cells grown in
212 UHCC00027 seeded (open symbols) or unseeded (closed symbols) PBRs in LC_HN
213 (squares, n = 2) or HC_LN (circles, n = 2 on days 2, 3, 5, 7, 10; n = 1 all others)
214 wastewater (Table 1) under room or cold (triangles) temperature (see Fig. S2). Growth
215 was also measured by dry cell weight (B, n = 1). The kinetics of changes in the culture
216 dry weight (C) and relationships of accumulation of total chlorophyll and dry weight
217 (D) are also presented. Data are presented as single measurements or the average of
218 duplicates with standard deviation.

219

220 This suggests that under the cold conditions, the indigenous algal-bacterial consortium
221 might have a competitive advantage over the introduced UHCC0027 algal cells in spite
222 of a low overall growth rate and in the absence of N limitation. It might be
223 advantageous to isolate and scale up the native consortium to test its applicability for
224 treatment of this kind of wastewater in future. Regardless of the experimental
225 conditions, a characteristic drop in culture biomass, measured as DW, was recorded in

the first five days of the experiment (Fig. 1C). The dramatic decline of DW coincided with abrupt decline of COD in the HC_LN reactors (Fig. 2A) but was not accompanied by a noticeable change in Chl content (Fig. 1A).

Starting from approximately day 5, there was pronounced biomass accumulation by the seeded PBRs operated at room temperature (Fig. 1C, curves *1* and *3*). The increase in biomass preceded the onset of the upward trend in Chl accumulation (Fig. 1A). In the cold PBR, a detectable increase in biomass was observed only after 12 days of operation, while Chl increased steadily from the beginning of the experiment (Fig 1A, C, curve *5*). At this phase, the increase in the culture DW was closely related to an increase in Chl content regardless of the temperature or the major nutrient ratio (Fig. 1A).

Collectively, the kinetics of biomass growth and accumulation of photosynthetic pigments (Chl) indicate a bi-phasic pattern of growth that is driven by the predominance of different organisms (Fig. 1D). The first phase is governed by the heterotrophic bacteria indigenous to the wastewater. The net result of this process was a rapid decline in the COD, essentially without participation of microalgal cells. The second phase is characterized by an exponential (linear in the case of the cold culture) growth of microalgae.

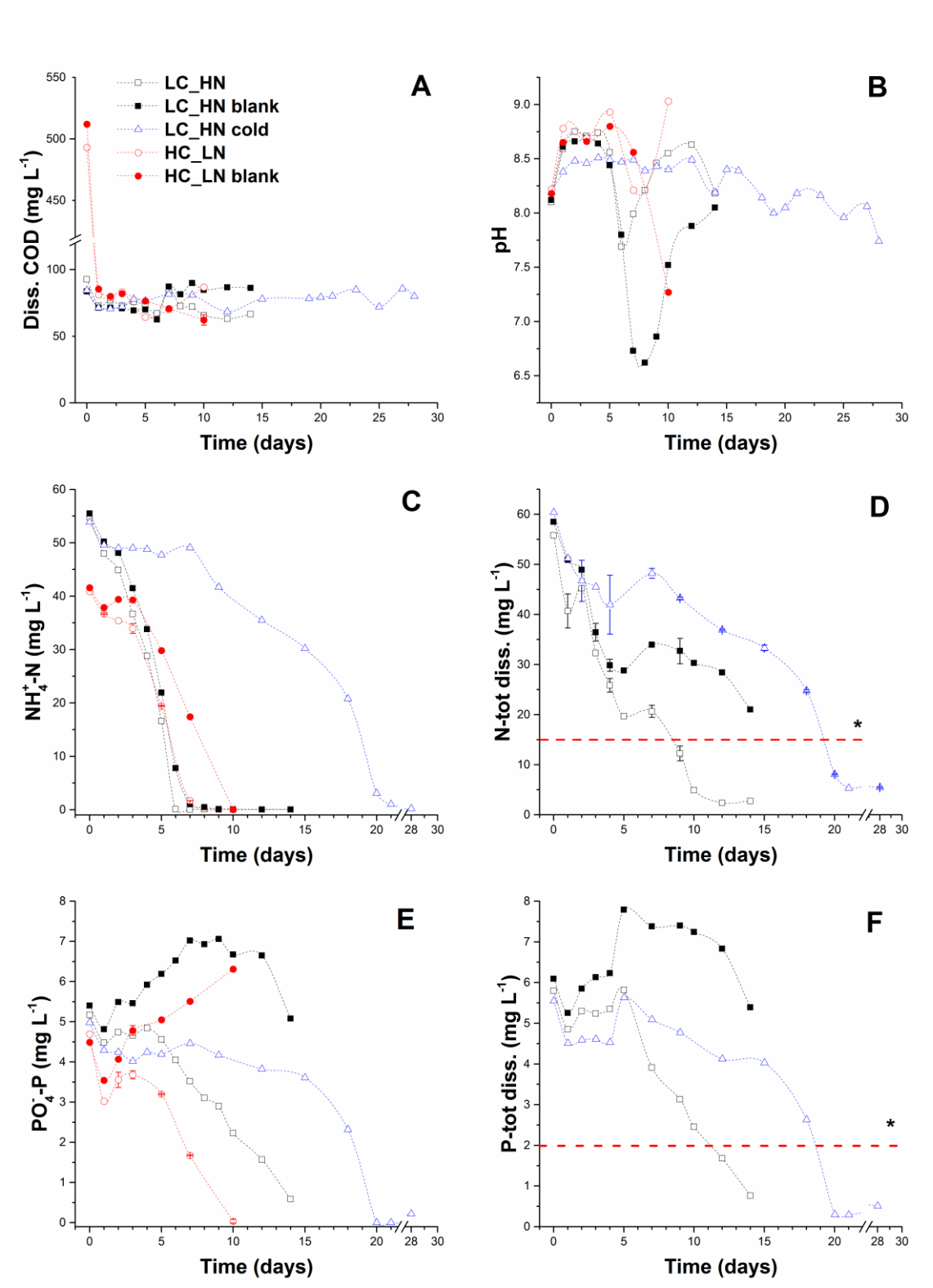

244

245 * UWWTD requirement for 10 000 - 100 000 population equivalent, 15 mg L^{-1} total N and 2
246 mg L^{-1} total P

Fig 2. Parameters characterizing wastewater treatment in the PBRs: Dissolved COD (A, n = 2 for HC_LN days 1, 3, 5, 7, 10; n = 1 all others), pH (B, n =1), ammoniacal nitrogen (C, n = 2 for HC_LN days 1,3,5,7,10; n = 1 all others), total dissolved nitrogen (D, n = 2, for LC_HN days 1, 4, 7, 9, 12, 15, 18, 20, 23, 25; n = 1 all others), inorganic phosphate (E, n = 2 for HC_LN days 2, 3, 5, 7, 10; n = 1 all others) and total dissolved phosphorous (F, n = 1) of UHCC0027 seeded (open symbols) and unseeded (closed symbols) PBRs in LC_HN (squares) or HC_LN (circles) wastewater (Table 1) under room or cold (triangles) temperatures (see Fig. S2). Data are presented as single measurements or the average of duplicates with standard deviation.

PBRs displayed distinct patterns of change in the pH of the wastewater (Fig. 2B). In unseeded PBRs a large drop in the wastewater pH was recorded at day 6 or 7, it was the highest in the LC_HN PBR, whereas it was modest in the HC_LN reactor. It is likely that these changes in pH resulted from the nitrification activity of bacteria in the absence of a notable growth of microalgae. In the reactors characterized by vigorous growth of microalgae, the pH was more or less stable around neutral, likely due to alkalization of the medium as a result of inorganic carbon uptake by microalgal cells.

3.1.2 Biological nutrient removal efficiency as a function of WW composition and cultivation conditions

The variable composition of the wastewater at different collection times allowed us to evaluate the performance of alga UHCC0027 under two different nutrient conditions, HC_LN and LC_HN (Table 1). While all of the pilot scale PBRs rapidly (within five days) met COD removal requirements of the EU Urban Waste Water Treatment Directive (UWWTD) 91/271/EEC [30], only the reactors seeded with UHCC0027 cells met the total N and P requirements (Fig. 2D & F). Overall, microalga UHCC0027

demonstrated a higher growth rate in the wastewater enriched in organics (HC_LN), the growth rate correlating with the efficiency of treatment. However, the difference in performance of UHCC0027 between the HC_LN and LC_HN conditions was small, demonstrating the robust performance of this alga.

The largest difference between the studied wastewater types were the COD and ammoniacal nitrogen concentrations (83.6 and 55.5 mg L^{-1} for the LC_HN and 493 and 41.6 mg L^{-1} and HC_LN, respectively; Fig. 2A & C). The HC_LN wastewater had a 5.9-fold higher starting COD level than the LC_HN (Table 1). Accordingly, the most dramatic decrease in the dissolved COD took place in the HC_LN within the first day of operation, resulting in a drop in dissolved COD concentration to that of LC_HN; the COD level did not change significantly thereafter (Fig. 2A). Such a rapid decrease in organic content was likely driven by fast growing heterotrophic bacteria indigenous to the wastewater [31], evidenced by transient but discernible peaks in the biomass accumulation curves of both seeded and unseeded HC_LN PBRs (Fig. 1C). It is also possible that (indigenous or seeded) microalgal cells capable of mixotrophic growth, contributed to both initial and subsequent decreases in COD.

Removal of total dissolved N and P was evaluated in LC_HN reactors to verify the fulfillment of UWWTD requirements at higher concentrations of total N and P. These requirements were met at hydraulic retention times (HRTs) of 9 and 12 days, for the seeded and unseeded PBRs respectively, whereas the cold climate HRT was 20 days (Fig. 2D & F). The room temperature HRTs are in the same range as batch experiments with similar initial nutrient loadings and cell densities as those summarized in Table 1 of Whitton et al. [32]. For example, the ‘medium’ cell density (1×10^6 cells mL^{-1}) experiment of Lau et al. [33], with initial loadings of 48.4 mg L^{-1} total Kjeldahl N

297 (TKN) and 4.29 mg L^{-1} total P, demonstrated 81.6% and 87% of TKN and total P
298 removed respectively after 10 days HRT. Phosphate removal was more rapid in the
299 HC_LN reactor where complete removal was achieved by day 10. This compares more
300 favorably with the medium cell density study of Lau et al. [33], which reached 92.8%
301 removal by day 10. Nevertheless, decreasing the observed HRTs would be desirable.
302 Seeding at a higher Chl concentration would decrease the algal nutrient load in the PBR
303 and would be a first step toward decreasing HRT. The next step would be to operate in a
304 continuous or semi-continuous mode, with chemostat operation shown to decrease
305 lengthy algal HRTs observed in batch mode [34].

306 Ammoniacal N was the major form of nitrogen present in the municipal wastewater
307 (80% of total dissolved N), with 33% more in the LC_HN than HC_LN wastewater
308 (Table 1; Fig. 2C & D). Algal uptake was demonstrated in both wastewaters by higher
309 rates of ammoniacal N removal in seeded versus unseeded reactors (Fig. 3A). However,
310 the differences between average removal rates between days 0 and 5 were small (7.6
311 and 6.7 mg L^{-1} d^{-1} *vs* 4.3 and 2.4 mg L^{-1} d^{-1} respectively), indicating that microalgal
312 uptake was not the major process driving ammoniacal N removal. Initial losses (day 1
313 and 2) of N from the reactor system, whereby ammoniacal, total dissolved and total N
314 all decreased and nitrate and nitrite levels remained close to zero can be explained by
315 ammonia air stripping, which is highly pH and temperature dependent and occurred to a
316 greater extent in the higher temperature LC_HN condition.

317 Nitrification was responsible for ammoniacal N removal once heterotrophic growth
318 slowed. This was evidenced by increased nitrite and nitrate concentrations and biomass
319 accumulation peaks in both seeded and unseeded reactors (Fig 1B, S4). Nitrification
320 appeared to be responsible for the majority of ammoniacal N removal in this study; the

oxygen required for this process was supplied by continuous aeration of the reactors. Nitrification rates were higher in the LC_HN reactors, possibly due to the higher temperatures and substrate concentrations. Despite the major role that nitrification played in N removal, the contribution made by seeded and indigenous algae is apparent in the positive correlation of dissolved inorganic nitrogen (DIN) removal with the accumulation of algal biomass (Fig. 3A). Seeding with UHCC00027 algae was necessary to achieve both phosphate and total dissolved phosphorous removal. Indeed, the unseeded reactors demonstrated net increases in P concentrations after the first day (Fig 2E & F). In the seeded PBRs operated at room temperature, approximately 100% and 90% (the HC_LN and LC_HN, respectively) phosphate removal was achieved after 14 days of the experiment.

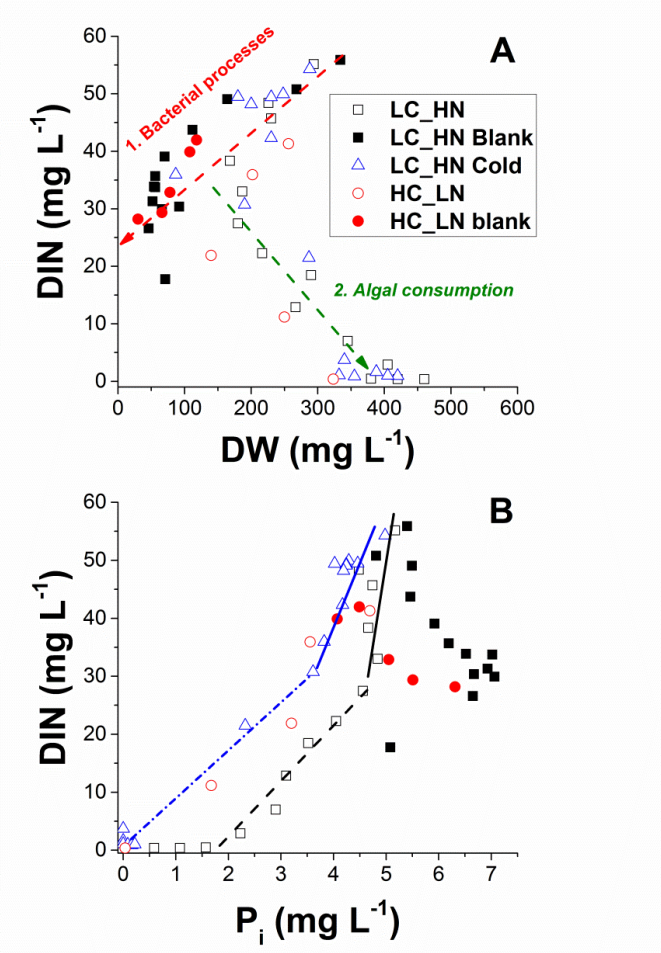

Fig. 3. Relationships between dissolved inorganic nitrogen (DIN, sum of NH_4^+-N, NO_2^--N and NO_3^--N) and dry weight (A) and between DIN and inorganic P (B) in PBRs seeded with alga UHCC00027 (open symbols) or unseeded (closed symbols) in LC_HN (squares) or HC_LN (circles) wastewater under room or cold (triangles) temperatures.

The lowest final phosphate concentration was recorded in the HC_LN reactor (0.04 mg L^{-1}). The slightly better algal growth rate in HC_LN was reflected in average phosphate removal rates, whereby a 36% faster removal rate was demonstrated between days 5 and 10. However, small overall differences between the reactors demonstrated the robust performance of the UHCC0027 alga over both wastewater compositions. Low phosphorus removal was demonstrated by UHCC0027 seeded under the cold condition

until day 7. However, an impressive removal rate was observed over days 15–20, when indigenous algal cells were rapidly growing. This resulted in the complete removal of phosphate and a final total dissolved phosphorous concentration of 0.3 mg L^{-1}.

3.1.3 UHCC0027 performance under cold climate conditions

The UHCC0027 alga was originally isolated from a coastal area of the Baltic Sea where the sea surface freezes most winters, indicating its potential for wastewater treatment under cold climate conditions. As temperatures in the cold PBR averaged approximately 15 °C below that in the corresponding LC_HN room temperature PBR (Fig. S2), delayed growth and nutrient removal were expected. Surprisingly, COD removal in the cold PBR was similar to that at room temperature (Fig. 2A) and biomass accumulation in exponential growth (delayed by 5−7 d under the cold condition) was only 1.3 times lower (35.3 vs. 45 mg L^{-1} d^{-1}) than under the room-temperature condition (Fig. 1C). Importantly, the cold PBR eventually met the UWWTD N and P removal targets, although HRTs were 2.1- and 1.4-fold longer than in the corresponding room-temperature PBR.

The lower N removal rates observed in the cold culture might stem from a temperature-dependent decline in ammonia air stripping [35] and nitrification [36]. This is consistent with other data demonstrating that the ammonia-oxidation step of nitrification is two times slower and nitrite oxidation rate more than three times slower when the temperature decreases from 25 °C to 10 °C [37,38].

Although the UHCC0027 pre-cultures were grown for 28 days at the same cold temperature, there was a considerable lag period before the algal cells started to grow in the PBR. It seems that the change to real wastewater in the PBR was a more stressful

environment to the microalgae under the cold condition. Interestingly, the microalgal cells in the cold PBR immediately started to accumulate Chl, although at a rate much slower than that recorded at room temperature (Fig. 1A). At the same time, there was no detectable nutrient uptake or biomass accumulation before day 6. It is possible that, rather than the active division of cells, this initial increase in Chl was due to the recovery of light-harvesting antenna damaged during the acclimation of cells to the cold pre-growth period.

After day 10, the PBR operated under the cold condition demonstrated robust biomass accumulation and nutrient removal performance. Remarkably, it also showed the highest maximum rate of phosphate removal (1.2 mg L^{-1} d^{-1} vs. 0.69 mg L^{-1} d^{-1} in the room temperature PBR). Differences in N:P ratio were likely behind this high rate, whereby P removal has previously been shown to improve under increased N concentration [39]. Although both reactors started with the same N:P ratio, the room temperature PBR demonstrated significant temperature-driven NH_3 stripping and nitrification, resulting in a more rapid removal of N than in the cold PBR. This effect is clear in the relationship of N and P removal rates presented in Fig. 3C, showing that N removal occurred four times faster than P removal (Fig. 3B). Both the cold and the unseeded room temperature PBRs displayed similar kinetics of Chl/DW accumulation (cf. curves *2* and *5*, Fig. 1B) and distinct trends of P removal (Fig. 2E and F), indicating that the indigenous algal consortium (acclimated to the composition of the wastewater and to the low growth temperature) outcompeted the seeded UHCC0027 alga in the cold PBR.

There have been very few studies of algal wastewater treatment and biomass accumulation under cold climate conditions. Most published reports have focused on

391 cold tolerant strains tested at laboratory scale in synthetic media [40]. Under such
392 conditions, rates of biomass accumulation at 10 °C ranged from 57 to 130 mg L^{-1} d^{-1}
393 [12, 41]. Rates in real wastewater, even on laboratory scale, have been lower at
394 approximately 32 to 50 mg L^{-1} d^{-1} [12]. Our pilot scale results using real wastewater,
395 were within this range at 35.3 mg L^{-1} d^{-1} on average, with a maximum rate of 50 mg L^{-1}
396 d^{-1} (Table S1). Much lower biomass accumulation rates of 5 mg L^{-1} d^{-1} were
397 demonstrated in a 10-fold larger scale study on hydroponics effluent performed in
398 Sweden, where the reactor temperature was close to 11 °C in the winter [42]. Under
399 these conditions, P removal rates were also much lower than those observed in our cold
400 PBR (maximum 1.2 mg L^{-1} d^{-1}; Table S1) with P precipitation playing a major role.
401 The P removal rates obtained in our study were comparable to those calculated from the
402 lab scale study of Tang et al. [24], where average and maximum removal rates were
403 0.56 and 0.71 mg L^{-1} d^{-1}, respectively, over 8 days at 10 °C for polar cyanobacteria and
404 a green algal assemblage. Also at lab scale, Chevalier et al. [43] reported much lower
405 maximum P removal rates of 0.6 mg L^{-1} d^{-1} at 15 °C for polar strains of cyanobacteria
406 and a fast-growing control strain (*P. bohneri*).

407

3.2 Biodiesel potential

Biomass samples were taken from pre-grown cells and from the LC_HN and LC_HN cold reactors at mid and late exponential growth phases and subjected to total lipid quantification and fatty acid (FA) profile analysis. The highest total lipid content (47% of cell DW) was recorded for biomass taken from the room temperature PBR on the final day of the LC_HN batch mode operation when N and P levels were the lowest (Fig. 4A). This value is typical of *Scenedesmus* cells grown under nutrient starvation [44–46].

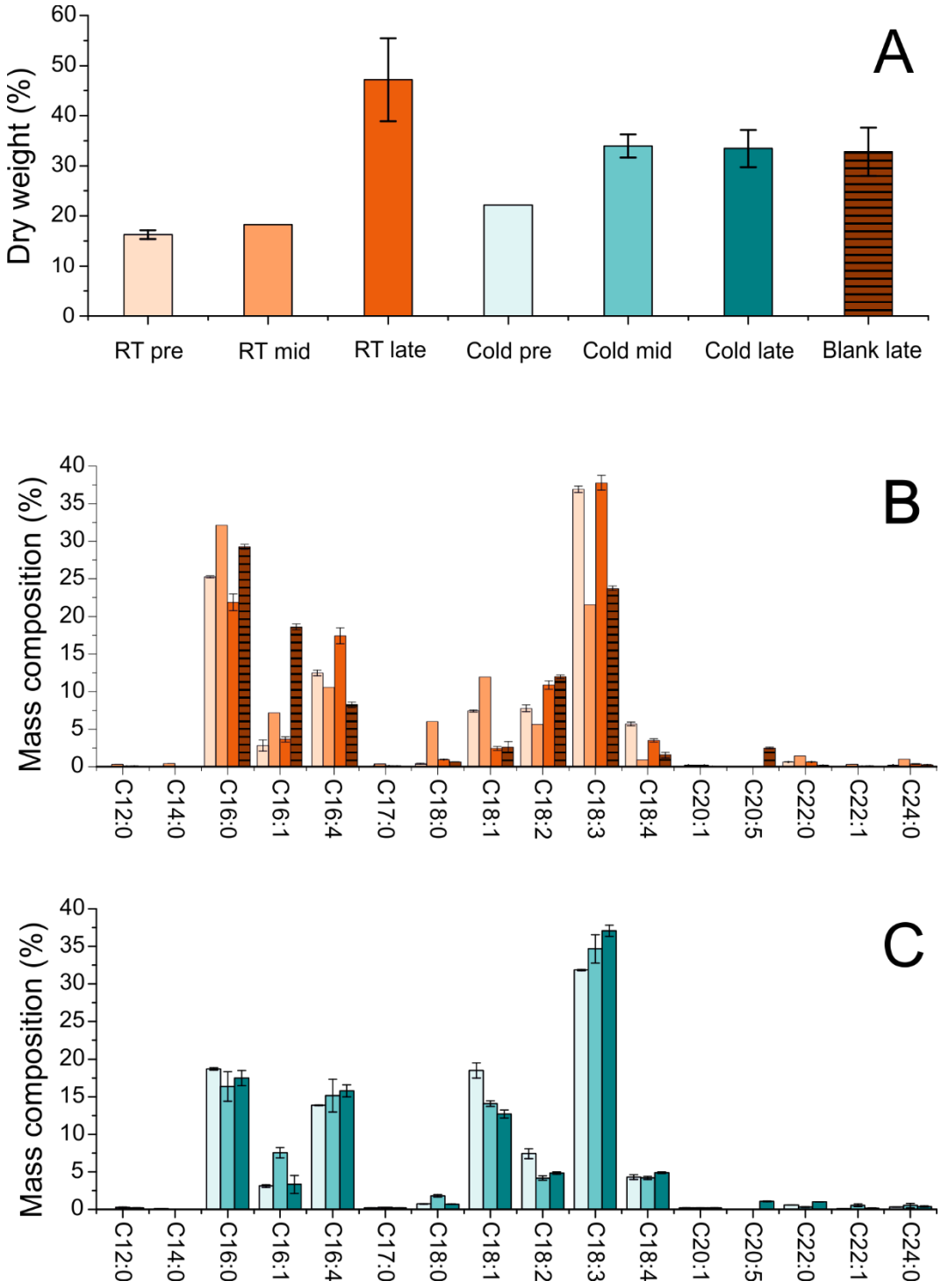

Fig. 4. Total cell lipid content (A, data are averages of n = 2 or 3 with standard deviations; n = 1 for mid phase and cold pre-growth) of biomass taken from exponentially growing pre-cultures (pre), and from mid and late exponential growth in the PBRs (LC_HN PBRs were operated at room and cold temperature, see Methods).

Fatty acid profiles of total lipids from different stages of the LC_HN experiment (B, data are averages of triplicates with standard deviations; n = 1 for LC_HN mid) and LC_HN cold experiment (C data are averages of triplicates with standard deviations; n = 2 for LC_HN cold pre).

3.2.1 Total lipid content

Conceivably, the exposure of microalgal cells to wastewater is stressful and can, among other effects, promote lipid accumulation [47,48]. However, this was not observed in UHCC0027 cells transferred from synthetic medium to real wastewater at room temperature, whereby the total-lipid content only increased 2%. Whilst it's possible that wastewater transfer induced stress was masked by pre-grown nutrient stressed cells, the total lipid content of pre-grown UHCC0027 cells was typical of rapidly dividing *Scenedesmus* [45,49], indicating that this was not likely the case. More likely, is the possibility of masking by the contribution of other wastewater indigenous organisms and particles with lower lipid contents to the total sampled biomass [50].

Interestingly, the transfer of cells from synthetic medium to real wastewater under the cold temperature resulted in a significant (12 %) increase in total lipids. This may be due to a slower division rate of cells which were already cold-stressed in the course of 28-days of pre-growth at the cold temperature. This suggestion is in line with the lower Chl content observed in these pre-culture cells [40]. The transfer of these cells to real wastewater could further exacerbate this stress (evident in the long lag period), inducing lipid accumulation as a side effect.

3.2.2 Fatty acid profile of total cell lipids

The most abundant FA found in the PBR-grown biomass were palmitate (C16:0) and α-

linolenate (C18:3; Fig. 4B & C), typical of other green algae including *Chlamydomonas*, *Chlorella*, and *Scenedesmus* [46,51]. The changes in these FA proportions demonstrated pronounced and opposite trends over the course of the room temperature experiment, whereby C16:0 peaked and C18:3 dropped at mid-exponential phase (Fig. 4B). An additional feature of the room temperature experiment was the presence of C18:0 FA in the mid-exponential cell lipids (5.7% vs. < 1% in the pre-cultures and late-exponential cells). Another FA obtained in high abundance from UHCC0027 cells was hexadecatetraenoic acid (C16:4) which is harbored by chloroplast thylakoid membrane glycolipids [52]. Such polyunsaturated FAs are not desirable in biodiesel due to their negative impact on cetane number (CN) and oxidative stability, but do hold potential as nutraceuticals. Interestingly, the FA profile of the mid-exponential phase biomass grown at room temperature appears to contain a higher composition of FA considered favorable for biodiesel performance than the pre-growth or late- phase samples. Whilst this sample was taken at what was estimated to be 'mid-exponential' growth (day 5), ammoniacal N had already been almost completely depleted (Fig. 2C) and the plot of Chl relative to dry weight (Fig. 1B, curve *1*) demonstrates that UHCC0027 cells had just reached stationary phase.

Cold temperature operation resulted in smaller changes in FA profiles than observed under room temperature conditions (Fig. 4C). The proportion of C18:3 FA, which is a typical glycolipid of chloroplast thylakoid membranes increased and that of C18:1 oleic acid, typical of neutral storage lipids [53], decreased slowly. The slow increase in C18:3/C18:1 ratio of the cold grown biomass over time might reflect the homeoviscous adaptation of cells to maintain membrane fluidity under cold conditions [54,55]. Considering the steady increase in Chl in the cold culture, the small changes in FA are

representative of the steady growth of algae limited only by the low growth temperature. These findings, together with a modest increase in total cell lipids (Fig. 4A) suggest a relatively low degree of actual stress in this culture [51].

Biomass obtained from the blank reactor, resulting from growth of indigenous microalgae and diatoms was enriched in C16:1 and demonstrated lower levels of C18:0. Interestingly, there were detectable amounts of the long chain polyunsaturated FA C20:5 in both the cold late phase lipids and in the blank (Fig. 4C), indicating possible accumulation of the omega-3 fatty acid Eicosapentaenoic acid (EPA) in the indigenous microalgae (Fig. S3).

Based on their FA profiles, the theoretical properties of the biodiesel from the PBR-grown microalgal biomass (Table 2) were predicted using the BiodieselAnalyzer© tool [28].

Table 2

Predicted properties of biodiesel from the biomass grown in the PBRs under room and cold temperature (see Methods).

		CFPP* (°C)	IV (g I_2)	CN	KV (υ) (mm^2 s^{-1})	Density (ρ) (g cm^{-3})	C18:3 ME (wt%)	Db ≥ 4 (wt%)	OS (h)
Standard EN 14214		≤ +5 – ≤ –5 (1 ≤ –5 – ≤ –26 (2	≤120	≥51	3.5 – 5.0	0.86–0.90	≤12	≤1	8
Standard ASTM D6751−02		-	-	≥47	1.9 – 6.0	-	-	-	-
Room temperature	pre	–4.2	186	31.9	3.36	0.888	35.0	18.1	5.3
	mid	12.9	128	45.0	3.74	0.880	19.6	11.4	7.3
	late	–3.7	203	28.0	3.23	0.890	36.2	20.9	5.1
	blank late	–3.9	147	40.3	3.53	0.883	22.7	12.3	6.0
Cold temperature	pre	–5.6	184	32.4	3.42	0.888	30.9	18.2	5.7
	mid	–4.6	191	30.8	3.35	0.889	33.6	19.3	5.7
	late	-4.1	202	28.3	3.29	0.890	36.2	21.7	5.5

1) Typical European summer values
2) Typical European winter values

* CFPP−cold filter plugging point (not included in standards), IV—iodine value, CN—cetane number, KV—kinematic viscosity, ME—methyl ester, Db—double bonds, OS—oxidative stability.

Oxidative stability was estimated according to Park et al. [29]. Cetane values and oxidative stability were relatively low for all samples due to high degrees of unsaturation, whereas CFPP values were within range for the same reason, with the exception of the room temperature exponential growth sample. In an evaluation of over

200 microalgal species (exponential growth, 18–25 °C), Stansell et al. [56] determined an average CN value of 42 for 24 Chlorophyceae species, which is close to our highest CN value of 45.

The biomass samples obtained in this study did not meet requirements set by the European Union or United States for biodiesel. However, this is a common shortcoming of microalgal biodiesel [56]. There are a number of workarounds for this issue, such as blending with diesel from other sources and/or adding antioxidants [20]. The cultivation regime can also be manipulated for the generation of biomass with altered FA profiles. For example, deprivation of the microalgal culture of N and a significantly longer incubation at stationary phase were shown to alter the FA profile of *Desmodesmus* sp. [57]. Since the UHCC0027 mid-exponential biomass grown at room temperature had the best FA profile from the standpoint of biodiesel production, it will be interesting to determine whether total N deprivation is required, or just deprivation of ammoniacal N. Also, a better FA profile was recorded when the algal cells had just reached stationary phase (day 5), *versus* late stationary phase (day 14) indicating that the HRT required for an improved FA profile could be optimized and balanced with wastewater treatment requirements.

Conclusions

This work is a novel evaluation of integrated wastewater treatment and lipid production by the locally isolated chlorophyte UHCC0027, using real municipal wastewater under varied nutrient and temperature regimes. Growth and nutrient removal of an indigenous algal-bacterial consortium was impressive, but seeding of UHCC0027 into pilot scale

PBRs was required to meet EU UWWTD requirements for N and P removal. N removal, including air stripping and nitrification processes, were strongly influenced by temperature, whereas P removal was influenced primarily by the variations in the N:P ratio. Microalgal PBR performance was demonstrated to be possible under a cold climate condition, with feasibility improving where the wastewater N:P ratio is favourable and an indigenous consortia can be established and supported. Lowering of the initial nutrient load on biomass (e.g. inoculation at a higher cell density) and/or switching of the PBRs to a (semi-) continuous turbidostat or chemostat operation mode are possible avenues for decreasing the HRT. The predicted properties of biodiesel from the PBR biomass fell short of current standards, but the results demonstrated that the cultivation regime can be manipulated for generation of biomass with improved suitability, for example at different N concentrations and HRTs.

Acknowledgments

This research was financially supported by the Kone Foundation and by the Academy of Finland FCoE program (307335) and mobility grant (287504). AS acknowledges the support of Russian Science Foundation (grant 14-50-00029).

References:

[1] Paris Agreement, (2016). https://treaties.un.org/pages/ViewDetails.aspx?src=TREATY&mtdsg_no=XXVII-7-d&chapter=27&lang=en (accessed June 30, 2016).

[2] European Commission, Climate actions: Energy, (2016). http://ec.europa.eu/clima/policies/international/paris_protocol/energy/index_en.htm (accessed August 3, 2016).

[3] R. van Noorden, EU debates U-turn on biofuels policy, Nature. (2013) 2–3. doi:10.1038/499013a.

[4] G. Dragone, B. Fernandes, A. Vicente, J. Teixeira, Third generation biofuels from microalgae, Curr. Res. Technol. Educ. Top. Appl. Microbiol. Microb. Biotechnol. (2010) 1355–1366. http://repositorium.sdum.uminho.pt/handle/1822/16807.

[5] F. Delrue, P. Álvarez-Díaz, S. Fon-Sing, G. Fleury, J.-F. Sassi, The Environmental Biorefinery: Using Microalgae to Remediate Wastewater, a Win-Win Paradigm, Energies. 9 (2016) 132. doi:10.3390/en9030132.

[6] S.R. Subashchandrabose, B. Ramakrishnan, M. Megharaj, K. Venkateswarlu, R. Naidu, Mixotrophic cyanobacteria and microalgae as distinctive biological agents for organic pollutant degradation, Environ. Int. 51 (2013) 59–72. doi:10.1016/j.envint.2012.10.007.

[7] X. Zhang, Microalgae removal of CO2 from flue gas, Clean Coal Technol. Res. Reports. (2015). http://bookshop.iea-coal.org.uk/reports/ccc-250/83697.

[8] G. Paswan, K. Nikhil, Biopurification of Waste Water Through Algaae – A Review, (2014) 71–73.

[9] All-gas, Description of the project, (2016). http://www.all-gas.eu/Pages/DescriptionofProject.aspx (accessed August 3, 2016).

[10] C.J. Willmott, S.M. Robeson, Climatologically aided interpolation (CAI) of terrestrial air temperature, Int. J. Climatol. 15 (1995) 221–229. doi:10.1002/joc.3370150207.

[11] M. Paulescu, E. Paulescu, P. Gravila, V. Badescu, Weather Modeling and Forecasting of PV Systems Operation, Green Energy Technol. 103 (2013). doi:10.1007/978-1-4471-4649-0.

[12] Abdelaziz, A. E., Leite, G. B., Belhaj, M. A., & Hallenbeck, P. C. (2014). Screening microalgae native to Quebec for wastewater treatment and biodiesel production. Bioresource technology, 157, 140-148.

[13] F.G. Gentili, Microalgal biomass and lipid production in mixed municipal, dairy, pulp and paper wastewater together with added flue gases, Bioresour. Technol. 169 (2014) 27–32. doi:10.1016/j.biortech.2014.06.061.

[14] F. Lynch, A. Santana-Sánchez, M. Jämsä, K. Sivonen, E.M. Aro, Y. Allahverdiyeva, Screening native isolates of cyanobacteria and a green alga for integrated wastewater treatment, biomass accumulation and neutral lipid production, Algal Res. 11 (2015) 411–420. doi:10.1016/j.algal.2015.05.015.

[15] Y. Chisti, Biodiesel from microalgae, Biotechnol. Adv. 25 (2007) 294–306. doi:http://dx.doi.org/10.1016/j.biotechadv.2007.02.001.

588 [16] Q. Hu, M. Sommerfeld, E. Jarvis, M. Ghirardi, M. Posewitz, M. Seibert, et al.,
589 Microalgal triacylglycerols as feedstocks for biofuel production: Perspectives and
590 advances, Plant J. 54 (2008) 621–639. doi:10.1111/j.1365-313X.2008.03492.x.

591 [17] E.M. Trentacoste, R.P. Shrestha, S.R. Smith, C. Gle, A.C. Hartmann, M.
592 Hildebrand, et al., Metabolic engineering of lipid catabolism increases microalgal
593 lipid accumulation without compromising growth, Proc. Natl. Acad. Sci. 110
594 (2013) 19748–19753. doi:10.1073/pnas.1309299110.

595 [18] M. Kumar, M.P. Sharma, Selection of potential oils for biodiesel production,
596 Renew. Sustain. Energy Rev. 56 (2016) 1129–1138.
597 doi:10.1016/j.rser.2015.12.032.

598 [19] G. Knothe, J.H. Van Gerpen, J.J. Krahl, J.H. Van Gerpen, The Biodiesel
599 Handbook, 2005. doi:10.1201/9781439822357.

600 [20] N. Ribeiro, A.C. Pinto, C.M. Quintella, G.O. da Rocha, L.S.G. Teixeira, L.L.N.
601 Guarieiro, et al., The role of additives for diesel and diesel blended (ethanol or
602 biodiesel) fuels: A review, Energy and Fuels. 21 (2007) 2433–2445.
603 doi:10.1021/ef070060r.

604 [21] P.V. Bhale, N. V. Deshpande, S.B. Thombre, Improving the low temperature
605 properties of biodiesel fuel, Renew. Energy. 34 (2009) 794–800.
606 doi:10.1016/j.renene.2008.04.037.

607 [22] R.J. Porra, W. A. Thompson, P.E. Kriedemann, Determination of Accurate
608 Extinction Coefficients and Simultaneous-Equations for Assaying Chlorophyll-a
609 and Chlorophyll-B Extracted with 4 Different Solvents - Verification of the

610 Concentration of Chlorophyll Standards by Atomic-Absorption Spectroscopy,
611 Biochim. Biophys. Acta. 975 (1989) 384–394. doi:Doi 10.1016/S0005-
612 2728(89)80347-0.

613 [23] APHA, A.P.H.A. and A.W. Works, Standard methods for the examination of
614 water and wastewater, APHA-AWWA-WEF, Washington, D.C., 2005.

615 [24] E.P.Y. Tang, W.F. Vincent, D. Proulx, P. Lessard, J. De la Noüe, Polar
616 cyanobacteria versus green algae for tertiary waste-water treatment in cool
617 climates, J. Appl. Phycol. 9 (1997) 371–381. doi:10.1023/A:1007987127526.

618 [25] E. Ryckebosch, K. Muylaert, I. Foubert, Optimization of an analytical procedure
619 for extraction of lipids from microalgae, JAOCS, J. Am. Oil Chem. Soc. 89
620 (2012) 189–198. doi:10.1007/s11746-011-1903-z.

621 [26] S. Van Wychen, L.M.L. Laurens, Determination of Total Lipids as Fatty Acid
622 Methyl Esters (FAME) by in situ Transesterification, NREL (Ed.) (2013) 275–
623 3000.

624 [27] H. Devle, E.O. Rukke, C.F. Naess-Andresen, D. Ekeberg, A GC - Magnetic
625 sector MS method for identification and quantification of fatty acids in ewe milk
626 by different acquisition modes, J. Sep. Sci. 32 (2009) 3738–3745.
627 doi:10.1002/jssc.200900455.

628 [28] A.F. Talebi, M. Tabatabaei, Y. Chisti, BiodieselAnalyzer© : a user-friendly
629 software for predicting the properties of prospective biodiesel, Biofuel Res. J. 2
630 (2014) 55–57.

631 [29] J. Park, D. Kim, J. Lee, S. Park, Y. Kim, J. Lee, Blending effects of biodiesels on

632 oxidation stability and low temperature flow properties, 99 (2008) 1196–1203.
633 doi:10.1016/j.biortech.2007.02.017.

634 [30] EEC Council, 91/271/EEC of 21 May 1991 concerning urban waste-water
635 treatment, EEC Counc. Dir. (1991) 10. doi:http://eur-lex.europa.eu/legal-
636 content/en/ALL/?uri=CELEX:31991L0271.

637 [31] C.P.L. Grady, Jr., G.T. Daigger, N.G. Love, C.D.M. Filipe, Biological
638 Wastewater Treatment, Third Edition, CRC Press, 2011.
639 https://books.google.com/books?hl=en&lr=&id=stjLBQAAQBAJ&pgis=1
640 (accessed February 18, 2016).

641 [32] R. Whitton, F. Ometto, M. Pidou, P. Jarvis, R. Villa, B. Jefferson, Microalgae for
642 municipal wastewater nutrient remediation: mechanisms, reactors and outlook for
643 tertiary treatment, Environ. Technol. Rev. 4 (2015) 133–148.
644 doi:10.1080/21622515.2015.1105308.

645 [33] P.S. Lau, N.F.Y. Tam, Y.S. Wong, Effect of algal density on nutrient removal
646 from primary settled wastewater, Environ. Pollut. 89 (1995) 59–66.
647 doi:10.1016/0269-7491(94)00044-E.

648 [34] P.J. McGinn, K.E. Dickinson, K.C. Park, C.G. Whitney, S.P. MacQuarrie, F.J.
649 Black, et al., Assessment of the bioenergy and bioremediation potentials of the
650 microalga Scenedesmus sp. AMDD cultivated in municipal wastewater effluent
651 in batch and continuous mode, Algal Res. 1 (2012) 155–165.
652 doi:10.1016/j.algal.2012.05.001.

653 [35] J. Arogo, R.H. Zhang, G.L. Riskowski, L.L. Christianson, D.L. Day, Mass

Transfer Coefficient of Ammonia in Liquid Swine Manure and Aqueous Solutions, J. Agric. Eng. Res. 73 (1999) 77–86. doi:10.1006/jaer.1998.0390.

[36] O.A.L.O. Saad, R. Conrad, Temperature dependence of nitrification, denitrification, and turnover of nitric oxide in different soils, Biol. Fertil. Soils. 15 (1993) 21–27. doi:10.1007/BF00336283.

[37] R. Blackburne, V.M. Vadivelu, Z. Yuan, J. Keller, Kinetic characterisation of an enriched Nitrospira culture with comparison to Nitrobacter, Water Res. 41 (2007) 3033–3042. doi:10.1016/j.watres.2007.01.043.

[38] J. Groeneweg, B. Sellner, W. Tappe, Ammonia oxidation in nitrosomonas at NH3 concentrations near km: Effects of pH and temperature, Water Res. 28 (1994) 2561–2566. doi:10.1016/0043-1354(94)90074-4.

[39] A. Beuckels, E. Smolders, K. Muylaert, Nitrogen availability influences phosphorus removal in microalgae-based wastewater treatment, Water Res. 77 (2015) 98–106. doi:10.1016/j.watres.2015.03.018.

[40] R.M. Morgan-kiss, J.C. Priscu, T. Pocock, L. Gudynaite-savitch, N.P.A. Huner, R.M. Morgan-kiss, et al., Adaptation and Acclimation of Photosynthetic Microorganisms to Permanently Cold Environments Adaptation and Acclimation of Photosynthetic Microorganisms to Permanently Cold Environments, Microbiol. Mol. Biol. Rev. 70 (2006) 222–252. doi:10.1128/MMBR.70.1.222.

[41] M.Y. Roleda, S.P. Slocombe, R.J.G. Leakey, J.G. Day, E.M. Bell, M.S. Stanley, Effects of temperature and nutrient regimes on biomass and lipid production by six oleaginous microalgae in batch culture employing a two-phase cultivation

676 strategy, Bioresour. Technol. 129 (2013) 439–49.
677 doi:10.1016/j.biortech.2012.11.043.

678 [42] K. Larsdotter, J.L.C. Jansen, G. Dalhammar, Phosphorus removal from
679 wastewater by microalgae in Sweden--a year-round perspective, Environ.
680 Technol. 31 (2010) 117–123. doi:10.1080/09593330903382815.

681 [43] P. Chevalier, D. Proulx, P. Lessard, W.F. Vincent, J. de la Noüe, Nitrogen and
682 phosphorus removal by high latitude mat-forming cyanobacteria for potential use
683 in tertiary wastewater treatment, J. Appl. Phycol. 12 (2000) 105–112.
684 doi:10.1023/A:1008168128654.

685 [44] L. Xin, H. Hong-ying, G. Ke, S. Ying-xue, Effects of different nitrogen and
686 phosphorus concentrations on the growth, nutrient uptake, and lipid accumulation
687 of a freshwater microalga Scenedesmus sp., Bioresour. Technol. 101 (2010)
688 5494–5500. doi:10.1016/j.biortech.2010.02.016.

689 [45] M.J. Griffiths, S.T.L. Harrison, Lipid productivity as a key characteristic for
690 choosing algal species for biodiesel production, J. Appl. Phycol. 21 (2009) 493–
691 507. doi:10.1007/s10811-008-9392-7.

692 [46] D. Schwenk, J. Seppälä, K. Spilling, A. Virkki, T. Tamminen, K.M. Oksman-
693 Caldentey, et al., Lipid content in 19 brackish and marine microalgae: Influence
694 of growth phase, salinity and temperature, Aquat. Ecol. 47 (2013) 415–424.
695 doi:10.1007/s10452-013-9454-z.

696 [47] O. Osundeko, A.P. Dean, H. Davies, J.K. Pittman, Acclimation of microalgae to
697 wastewater environments involves increased oxidative stress tolerance activity,

698 Plant Cell Physiol. 55 (2014) 1848–1857. doi:10.1093/pcp/pcu113.

699 [48] A. Polishchuk, D. Valev, M. Tarvainen, S. Mishra, V. Kinnunen, T. Antal, et al.,
700 Cultivation of Nannochloropsis for eicosapentaenoic acid production in
701 wastewaters of pulp and paper industry, Bioresour. Technol. 193 (2015) 469–
702 476. doi:10.1016/j.biortech.2015.06.135.

703 [49] G.H. Gim, J.K. Kim, H.S. Kim, M.N. Kathiravan, H. Yang, S.H. Jeong, et al.,
704 Comparison of biomass production and total lipid content of freshwater green
705 microalgae cultivated under various culture conditions, Bioprocess Biosyst. Eng.
706 37 (2014) 99–106. doi:10.1007/s00449-013-0920-8.

707 [50] M. Cea, N. Sangaletti-Gerhard, P. Acuña, I. Fuentes, M. Jorquera, K. Godoy, et
708 al., Screening transesterifiable lipid accumulating bacteria from sewage sludge
709 for biodiesel production, Biotechnol. Reports. 8 (2015) 116–123.
710 doi:10.1016/j.btre.2015.10.008.

711 [51] M.L. Teoh, S.M. Phang, W.L. Chu, Response of Antarctic, temperate, and
712 tropical microalgae to temperature stress, J. Appl. Phycol. 25 (2013) 285–297.
713 doi:10.1007/s10811-012-9863-8.

714 [52] E.H. Harris, The Chlamydomonas Sourcebook, Academic Press Inc., San Diego,
715 CA, 1989.

716 [53] G.A. Thompson, Lipids and membrane function in green algae, Biochim.
717 Biophys. Acta - Lipids Lipid Metab. 1302 (1996) 17–45. doi:10.1016/0005-
718 2760(96)00045-8.

719 [54] J.R. Hazel, Thermal Adaptation in Biological Membranes: Is Homeoviscous

720 Adaptation the Explanation?, Annu. Rev. Physiol. 57 (1995) 19–42.
721 doi:10.1146/annurev.ph.57.030195.000315.

722 [55] D.A. Los, N. Murata, Membrane fluidity and its roles in the perception of
723 environmental signals, Biochim. Biophys. Acta - Biomembr. 1666 (2004) 142–
724 157. doi:10.1016/j.bbamem.2004.08.002.

725 [56] G.R. Stansell, V.M. Gray, S.D. Sym, Microalgal fatty acid composition:
726 Implications for biodiesel quality, J. Appl. Phycol. 24 (2012) 791–801.
727 doi:10.1007/s10811-011-9696-x.

728 [57] A.E. Solovchenko, O.A. Gorelova, O.I. Baulina, I.O. Selyakh, L.R. Semenova,
729 O.B. Chivkunova, et al., Physiological plasticity of symbiotic Desmodesmus
730 (Chlorophyceae) isolated from taxonomically distant white sea invertibrates,
731 Russ. J. Plant Physiol. 62 (2015) 653–663. doi:10.1134/S1021443715050167.

732